

Analysis and Predictive Modeling of Solar Coronal Holes Using Computer Vision and ARIMA-LSTM Networks

Juyoung Yun^{1*}, Jungmin Shin²

¹Stony Brook University, New York, USA

²Defense Acquisition Program Administration (DAPA), Gwacheon-si, Republic of Korea

Abstract

In the era of space exploration, coronal holes on the sun play a significant role due to their impact on satellites and aircraft through their open magnetic fields and increased solar wind emissions. This study employs computer vision techniques to detect coronal hole regions and estimate their sizes using imagery from the Solar Dynamics Observatory (SDO). Additionally, we utilize hybrid time series prediction model, specifically combination of Long Short-Term Memory (LSTM) networks and ARIMA, to analyze trends in the area of coronal holes and predict their areas across various solar regions over a span of seven days. By examining time series data, we aim to identify patterns in coronal hole behavior and understand their potential effects on space weather.

1 Introduction

The exploration of space has underscored the importance of understanding space weather phenomena, especially those related to coronal holes (Davis 1990; Sandford 1999). These regions on the sun, characterized by open magnetic field lines and cooler temperatures, emit solar winds at higher rates than their surroundings. Such emissions have profound implications for Earth, influencing operations of aircraft, satellites, and terrestrial technologies (Filjar and Kos 2006; Rao et al. 2009).

Space weather affects the expanse between the Sun and Earth, impacting the solar wind, Earth's magnetosphere, ionosphere, and thermosphere (Oceanic and Administration). Phenomena like solar flares and coronal mass ejections shape space weather, causing disruptions in satellite communications and GPS accuracy (Schwenn 2006; Rao et al. 2009). While coronal holes' influence on space weather is well-known, predicting their size and evolution remains a challenge. Accurate prediction of coronal hole areas is crucial, as their size and position can directly affect the intensity and impact of solar wind streams (Kappenman 1996; Boteler 2013).

Addressing this gap, our study combines computer vision with deep learning to predict coronal hole sizes. Automated detection ensures accuracy and consistency, eliminating manual inspection errors, and enhancing efficiency. Using the

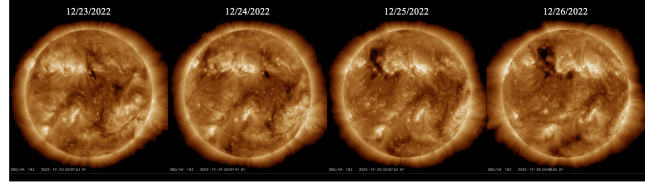


Figure 1: A visual representation of the changes in coronal hole size and position over a 4-day period from December 23, 2022 to December 26, 2022 (NASA). The image illustrates the dynamic nature of coronal holes and their potential impact on space weather events.

Long Short-Term Memory (LSTM) model (Hochreiter and Schmidhuber 1997) and ARIMA (Box and Jenkins 1970), we forecast coronal hole sizes over a week, providing insights into impending space weather events. Our scalable method allows for extensive dataset analysis, offering insights into long-term coronal hole patterns. This research highlights the critical role of AI in enhancing predictive capabilities for space weather events, ultimately protecting Earth's technological infrastructure (Oceanic and Administration).

2 Related Works

In space weather studies, observing coronal holes is essential. These features are visible using extreme ultraviolet (EUV) wavelengths and are monitored by instruments like the AIA on the Solar Dynamics Observatory (SDO) (Lemen et al. 2012; NASA). Computational models such as MHD and potential field source surface (PFSS) models help detect these holes by simulating the sun's magnetic field and plasma behavior (Inoue 2016). Coronal mass ejections (CMEs) and corotating interaction regions (CIRs) from varying speed solar wind streams can induce geomagnetic storms, impacting Earth's space environment (Webb and Howard 2012; Schwenn 2006; Heber, Sanderson, and Zhang 1999; Mursula and Zeiger 1996; Bobrov 1983; Richardson, Cliver, and Cane 2000, 2001). Geomagnetic activity is measured using indices like K_p, AE, and D_{st}, which help assess the intensity and effects of these storms (Carley, Vilmer, and Vourlidas 2020; Filjar and Kos 2006; Rao et al. 2009; Badruddin and Falak 2016; Bartels 1949, 1938; Cranmer 2009; NOAA). Historically, research has focused on detecting coronal holes using

*Corresponding author. E-Mail: juyyun@cs.stonybrook.edu
This paper is accepted to the first joint European Space Agency SPAICE Conference 2024. <https://spacie.esa.int/>

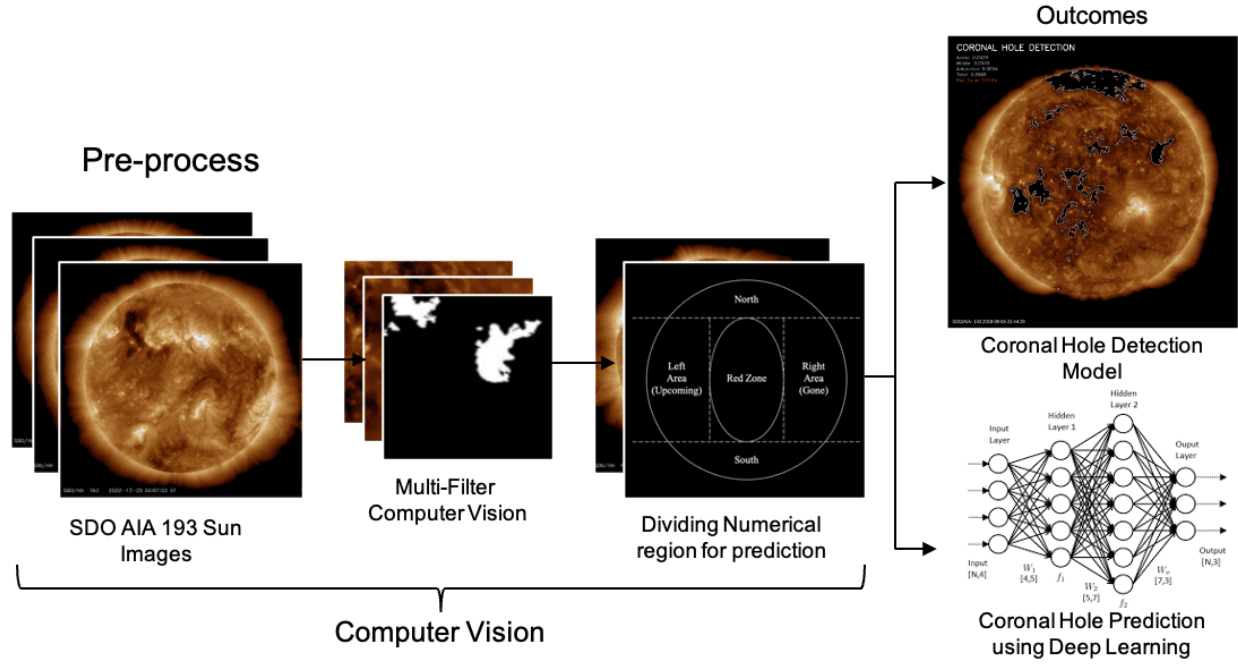


Figure 2: Overall structure of the predictive modeling of coronal hole areas using computer vision and deep learning. The regions used to determine the coronal hole area on the sun are defined by the binary-based Coronal Hole Detection (BCH) model with AIA-193 (NASA).

various techniques from manual inspection to advanced computer vision (Linker et al. 2021; Jarolim et al. 2021). While these methods improved detection accuracy, they did not predict future behavior. Our study addresses this gap by combining detection with prediction, using the LSTM (Hochreiter and Schmidhuber 1997) model to forecast coronal hole area over a seven-day period. This advancement enhances our ability to prepare for space weather events in the future.

3 Methodology

We develop a novel approach to predict the area of coronal holes by utilizing computer vision and deep learning. Our methodology consists of two primary phases: detecting coronal holes through computer vision and predicting their future area using deep learning as depicted in Figure 2.

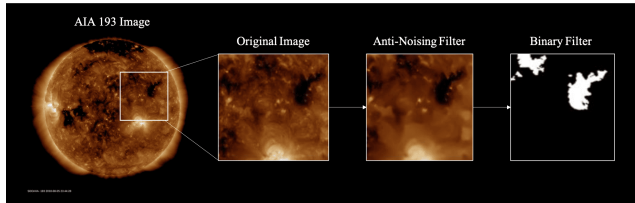


Figure 3: A depiction of the multi-filters computer vision based detection applied to an original AIA 193 image (NASA), including anti-noising and binary filters to accurately identify and measure coronal holes in the sun.

3.1 Coronal Hole Detection using Computer Vision

Our study employs advanced and simple computer vision techniques to automate the detection of coronal holes without any training deep learning model, utilizing methods like the non-local means (NLmeans) for enhancing image clarity and reducing noise, making features of coronal holes more distinguishable (Buades, Coll, and Morel 2005) as shown in Figure 3. Subsequently, we apply image binarization to transform the processed images into a binary format that highlights the coronal holes against the solar background (Gonzalez and Woods 2006). This step is crucial for accurately delineating the boundaries of coronal holes. Finally, we refine our detection using the Laplacian of Gaussian (LOG) method, which is sensitive to abrupt changes in image intensity, aiding in precise contour detection of the coronal holes (Marr 1980). This comprehensive approach ensures accurate identification and analysis of coronal hole regions.

In our segmentation, the middle region, which includes the Left Area, Redzone, and Right Area, generally involves areas close to the solar equator, potentially extending to about $\pm 30^\circ$ latitude from the solar equator as shown in Figure 2. These regions are more likely to impact Earth's geomagnetic environment directly due to their equatorial proximity.

Specifically, the Redzone is defined within a 15° wide longitudinal slice around the heliocentric meridian and falls within $\pm 30^\circ$ latitude from the solar equator (Nakagawa, Nozawa, and Shinbori 2019). Areas outside of this middle region are classified as polar regions. Additionally, for quan-

titative analysis, we calculate the percentage of the white area (coronal holes) relative to the total solar surface area, considering the entire solar area as a unity 1.

Coronal Hole Analysis Before diving into deep learning predictions, it's essential to focus on data extraction and preprocessing. Our work with the Binary-based Coronal Hole Detection (BCH) model ensures the data is accurate and meaningful, providing a strong foundation for deep learning applications.

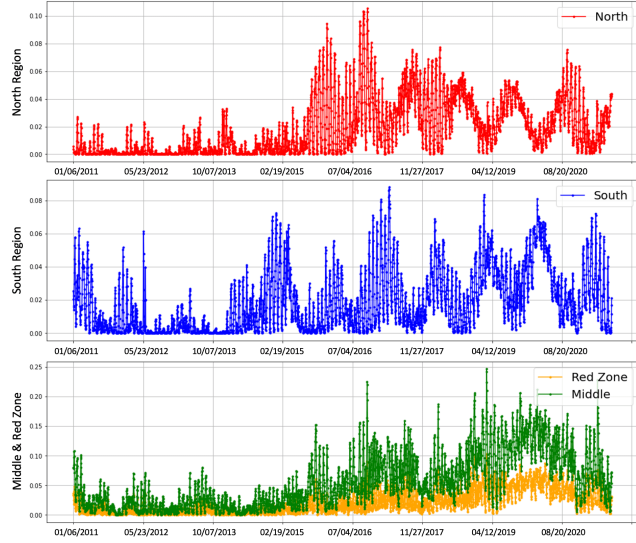


Figure 4: Daily coronal hole data for each region of the sun over 3857 days from January 6, 2011, to August 10, 2021, as detected by the BCH model. The graph shows the variation in coronal hole area over time.

Overall. Figure 4 shows the expansion of coronal hole areas over time, particularly from January 6, 2011, to August 10, 2021. The middle region of the sun has seen a significant increase, suggesting a trend that requires longer-term data for a comprehensive understanding.

Middle Region. Our analysis indicates a correlation between the size of coronal holes in the middle region and redzone and geomagnetic disturbances on Earth, as measured by the AP index. Figure 5 highlights this relationship over a 50-day period, showing that increases in the size of the middle region often precede rises in the AP index. This finding is consistent with previous research suggesting that severe coronal holes in the middle region can impact Earth's geomagnetic environment within 3-5 days (Watari, Nakamizo, and Ebihara 2023).

Polar Region. The polar regions of the sun also exhibit distinct behaviors, as shown in Figure 6. The "polarity rule" demonstrates that coronal hole areas at the north and south poles often behave oppositely, aligning with their magnetic field configurations and affecting solar wind distribution. These findings emphasize the importance of continuous monitoring and further research to understand the long-term impacts of coronal holes on space weather and geomagnetic disturbances on Earth.

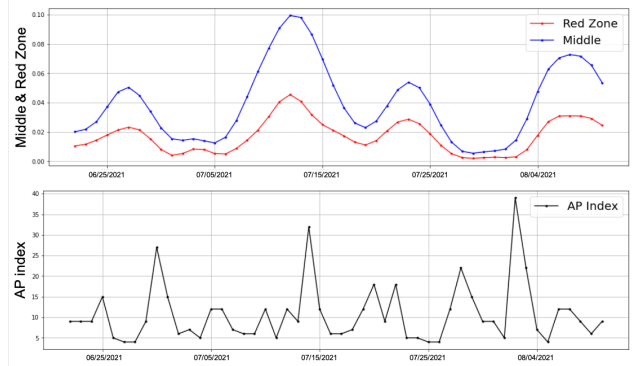


Figure 5: The AP index and coronal hole areas in the middle and redzone regions of the sun from June 22, 2021, to August 10, 2021, as detected by the BCH model. The graph shows the correlation between the AP index and coronal hole area in these regions.

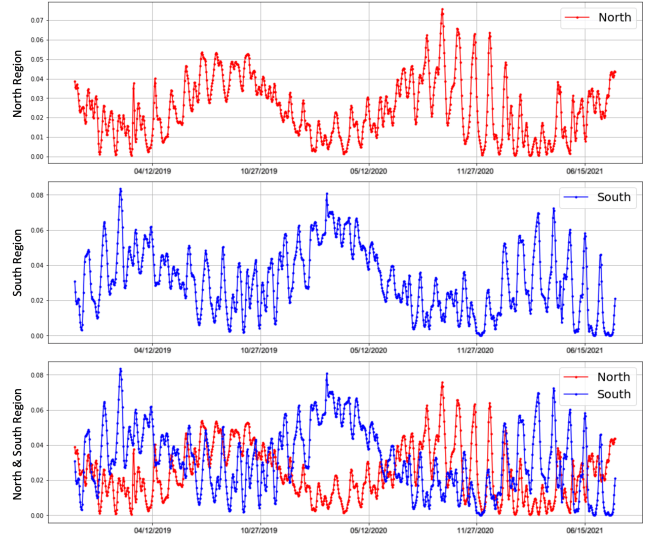


Figure 6: Daily coronal hole data for the sun's south and north regions over 1000 days from November 13, 2018, to August 10, 2021, as detected by the BCH model. The graph shows the variation in coronal hole area and the consistency of the polarity rule.

3.2 Time Series Prediction using Deep Learning

In our study, we integrate Long Short-Term Memory (LSTM) networks (Hochreiter and Schmidhuber 1997) with AutoRegressive Integrated Moving Average (ARIMA) (Box and Jenkins 1970) models to predict the future behavior of coronal holes. LSTM networks efficiently manage long-term dependencies in data, crucial for accurate time series predictions (Yang et al. 2019; Torres, Martínez-Álvarez, and Troncoso 2022). Additionally, we use the `pm.auto_arima` function from the `pmdarima` library (Smith et al. 2019) to automatically determine the best fitting parameters for the ARIMA model. For our predictions, we generate forecasts from both

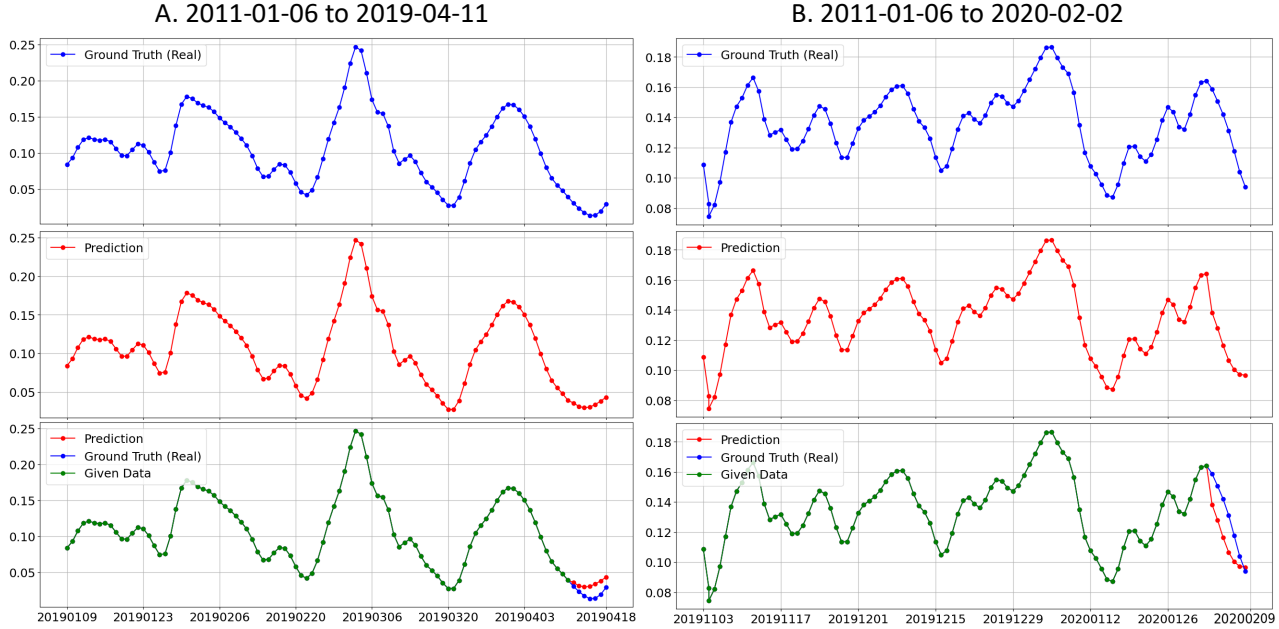


Figure 7: The plots from A to B show the ARIMA-LSTM predicted the next 7 days of middle area of coronal holes. Each plot corresponds to a different time period used for training: (A) 2011-01-06 to 2019-04-11, (B) 2011-01-06 to 2020-02-02. The blue lines indicate the actual coronal hole areas used for training and the actual areas for the following 7 days. The red lines show the predicted areas for the next 7 days based on the given training data. The green lines represent the data used for training. This visualization highlights the effectiveness of the ARIMA-LSTM hybrid model in predicting the future behavior of coronal holes.

the ARIMA and LSTM models over a 7-day period and then compute the average of these predictions to obtain the final forecasted values. This hybrid approach enhances the overall prediction accuracy by leveraging the strengths of both models.

4 Results

4.1 Experimental Setting

In our study, we employed a Long Short-Term Memory (LSTM) network to predict the future behavior of coronal holes. The LSTM model architecture consists of an initial LSTM layer with 50 units and a ReLU activation function, configured to return sequences. This is followed by a Dropout layer with a dropout rate of 0.2 to prevent overfitting. Next, there is another LSTM layer with 50 units and a ReLU activation function, which does not return sequences. Another Dropout layer with a dropout rate of 0.2 is added, and the final layer is a Dense layer with a single unit for the output. The model is compiled using the mean squared error (MSE) loss function and the Adam optimizer, with the learning rate set to the default value. The model was trained for 50 epochs with a batch size of 128 and a learning rate of 0.01.

4.2 Experimental Results

We employ ARIMA-LSTM (Hochreiter and Schmidhuber 1997; Box and Jenkins 1970) networks to predict the area of coronal holes in the sun's middle region. The LSTM model, trained on 3857 days of numerical data from the middle

regions of AIA 193 observations extracted by the BCH model, is adept at handling time-series data, capturing patterns and trends in solar activity.

Figure 7, 8 illustrates the performance of the ARIMA-LSTM hybrid model in predicting the Daily middle area of coronal holes for the next 7 days. The model is trained on different time periods, as shown in plots A to D, which cover various spans from 2011-01-06 to 2021-03-06. The blue lines represent the actual coronal hole areas used for training and the actual areas for the subsequent 7 days. The red lines indicate the predicted areas for the next 7 days based on the training data, and the green lines represent the data used for training.

The patterns observed in the coronal hole areas suggest that these features exhibit specific trends and behaviors over time. By leveraging these patterns, the ARIMA-LSTM hybrid model can effectively learn and predict future coronal hole areas. This approach demonstrates that it is possible to accurately predict the behavior of coronal holes based on their historical patterns, providing valuable insights for understanding and forecasting space weather phenomena.

5 Discussion

This study enhances understanding of coronal holes and their impacts on space weather by developing a detection and prediction model. While effective, the model focuses mainly on mid-zone areas, neglecting variations in regions like the polar regions which might influence space weather. Additionally, it covers only one solar cycle, limiting its scope. Future

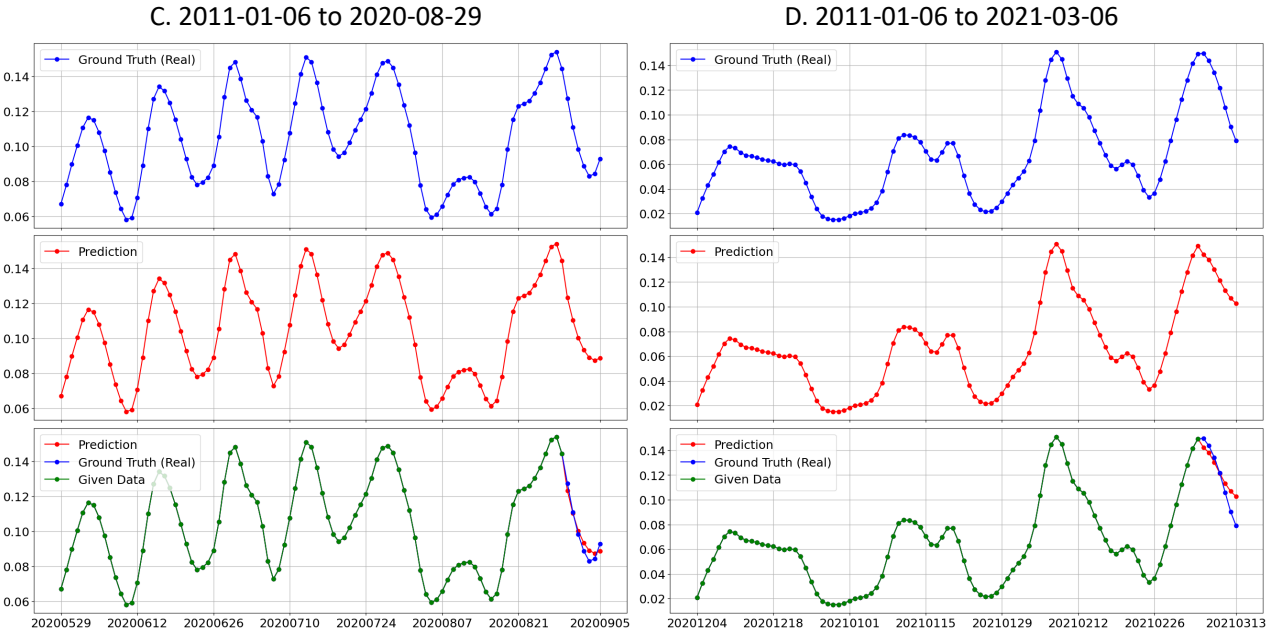


Figure 8: The plots from C to D show the ARIMA-LSTM predicted the next 7 days of middle area of coronal holes. Each plot corresponds to a different time period used for training: (C) 2011-01-06 to 2020-08-29, (D) 2011-01-06 to 2021-03-06. The blue lines indicate the actual coronal hole areas used for training and the actual areas for the following 7 days. The red lines show the predicted areas for the next 7 days based on the given training data. The green lines represent the data used for training. This visualization highlights the effectiveness of the ARIMA-LSTM hybrid model in predicting the future behavior of coronal holes.

research should delve deeper into the physical processes governing coronal hole formation, particularly the sun's magnetic dynamics.

6 Conclusion

A simplified model for detecting coronal holes is essential for enhancing space weather forecasting. Coronal holes, marked by their low temperature and density, influence solar winds that can affect Earth's satellites and power grids. Accurate detection and measurement of coronal holes are crucial for predicting space weather events and mitigating their impacts. Our research developed a model that identifies coronal holes, generating 3857 data entries. This data was used to create a deep learning prediction model, specifically using ARIMA-LSTM, to estimate the size of coronal holes. The model showed promising results, effectively predicting the coronal hole size using numerical data. This model improves our ability to predict space weather events, aiding in the prevention of potential impacts on Earth's technological infrastructure. Additionally, understanding the size and location of coronal holes helps in predicting solar activities like CMEs and CIRs.

References

Badruddin; and Falak, Z. 2016. Study of the geoeffectiveness of coronal mass ejections, corotating interaction regions and their associated structures observed during Solar Cycle 23. *Astrophysics and Space Science*, 361(8): 253–316.

Bartels, J. 1938. Potsdamer erdmagnetische Kennziffern, 1. Mitteilung. *Zeitschrift für Geophysik*, 14: 68–78.

Bartels, J. 1949. The standardized index, K_s , and the planetary index, K_p . *IATME Bulletin*, 12b: 97–120.

Bobrov, M. S. 1983. Non-recurrent geomagnetic disturbances from high-speed streams. *Planetary and Space Science*, 31: 865.

Boteler, D. 2013. Space Weather Effects on Power Systems. *Geophysical Monograph Series*, 125: 347–352.

Box, G. E. P.; and Jenkins, G. M. 1970. *Time Series Analysis: Forecasting and Control*. San Francisco, CA: Holden-Day.

Buades, A.; Coll, B.; and Morel, J. M. 2005. A non-local algorithm for image denoising. In *2005 IEEE Computer Society Conference on Computer Vision and Pattern Recognition (CVPR'05)*, volume 2, 60–65.

Carley, E. P.; Vilmer, N.; and Vourlidas, A. 2020. Radio Observations of Coronal Mass Ejection Initiation and Development in the Low Solar Corona. *Frontiers in Astronomy and Space Sciences*, 7: 79.

Cranmer, S. R. 2009. Coronal Holes. *Living Reviews in Solar Physics*, 6: 3.

Davis, K. 1990. *Ionospheric Radio*. London, UK: Peter Peregrinus Ltd.

Filjar, R.; and Kos, T. 2006. GPS Positioning Accuracy in Croatia during the Extreme Space Weather Conditions in September 2005. In *European Navigation Conference ENC 2006*. Manchester, UK.

Gonzalez, R. C.; and Woods, R. E. 2006. *Digital Image Processing*. Boston, MA: Pearson Education, 3rd edition.

Heber, B.; Sanderson, T. R.; and Zhang, M. 1999. Corotating interaction regions. *Advances in Space Research*, 23(3): 567–579.

Hochreiter, S.; and Schmidhuber, J. 1997. Long Short-Term Memory. *Neural Computation*, 9(8): 1735–1780.

Inoue, S. 2016. Magnetohydrodynamics modeling of coronal magnetic field and solar eruptions based on the photospheric magnetic field. *Prog. in Earth and Planet. Sci.*, 3: 19.

Jarolim, R.; Veronig, A. M.; Hofmeister, S.; Heinemann, S. G.; Temmer, M.; Podladchikova, T.; and Dissauer, K. 2021. Multi-channel coronal hole detection with convolutional neural networks. *Astronomy & Astrophysics*, 652: A13.

Kappenman, J. G. 1996. Geomagnetic storms and their impact on power systems. *IEEE Power Engineering Review*, 16(5): 46–53.

Lemen, J. R.; Title, A. M.; Akin, D. J.; et al. 2012. The Atmospheric Imaging Assembly (AIA) on the Solar Dynamics Observatory (SDO). *Solar Physics*, 275: 17–40.

Linker, J. A.; Heinemann, S. G.; Temmer, M.; Owens, M. J.; Caplan, R. M.; Arge, C. N.; Asvestari, E.; Delouille, V.; Downs, C.; and Hofmeister, S. J. 2021. Coronal Hole Detection and Open Magnetic Flux. *The Astrophysical Journal*, 918(1): 21.

Marr, D. 1980. Theory of edge detection. *Proceedings of the Royal Society of London B: Biological Sciences*, 207(1167): 187–217.

Mursula, K.; and Zeiger, B. 1996. The 13.5-day periodicity in the sun, solar wind, and geomagnetic activity: The last three solar cycles. *Journal of Geophysical Research*, 101: 27,077.

Nakagawa, Y.; Nozawa, S.; and Shinbori, A. 2019. Relationship between the low-latitude coronal hole area, solar wind velocity, and geomagnetic activity during solar cycles 23 and 24. *Earth Planets Space*, 71: 24.

NASA. ???? Solar Dynamics Observatory (SDO). Retrieved from <https://sdo.gsfc.nasa.gov/>.

NOAA. ???? AP index. Retrieved from <https://www.swpc.noaa.gov/products/geospace-indices>.

Oceanic, N.; and Administration, A. ???? Space weather. Retrieved from <https://www.noaa.gov/education/resource-collections/space-weather>.

Rao, P. V. S. R.; Krishna, S. G.; Prasad, J. V.; Prasad, S. N. V. S.; Prasad, D. S. V. V. D.; and Niranjan, K. 2009. Geomagnetic storm effects on GPS based navigation. *Ann. Geophys.*, 27: 2101–2110.

Richardson, I. G.; Cliver, E. W.; and Cane, H. V. 2000. Sources of magnetic activity over the solar cycle: Relative importance of coronal mass ejections, high-speed streams, and slow solar wind. *Journal of Geophysical Research*, 105: 18,203.

Richardson, I. G.; Cliver, E. W.; and Cane, H. V. 2001. Sources of geomagnetic storms for solar minimum and maximum conditions during 1972–2000. *Geophysical Research Letters*, 28: 2569.

Sandford, W. H. 1999. The Impact on Solar Winds on Navigation Aids. *The Journal of Navigation*, 52: 42–46.

Schwenn, R. 2006. Space Weather: The Solar Perspective. *Living Reviews in Solar Physics*, 3(2).

Smith, T. G.; Greenberg, D. S.; Radcliffe, N.; and Grant, T. 2019. pmdarima: ARIMA estimators for Python. Version 1.5.3.

Torres, J. F.; Martínez-Álvarez, F.; and Troncoso, J. 2022. A deep LSTM network for the Spanish electricity consumption forecasting. *Neural Computing & Applications*, 34: 10533–10545.

Watari, S.; Nakamizo, A.; and Ebihara, Y. 2023. Solar events and solar wind conditions associated with intense geomagnetic storms. *Earth, Planets and Space*, 75(1): 90.

Webb, D. F.; and Howard, T. A. 2012. Coronal Mass Ejections: Observations. *Living Reviews in Solar Physics*, 9(3).

Yang, B.; Sun, S.; Li, J.; Lin, X.; and Tian, Y. 2019. Traffic flow prediction using LSTM with feature enhancement. *Neurocomputing*, 332: 320–327.